

Comparative Analysis of Kinetic Realizations of Insulin Signaling

Patrick Vincent N. Lubenia¹, Eduardo R. Mendoza^{1,2,3}, and Angelyn R. Lao^{1,2,4*}

¹*Systems and Computational Biology Research Unit, Center for Natural Sciences and Environmental Research, 2401 Taft Avenue, Manila, 0922, Metro Manila, Philippines*

²*Department of Mathematics and Statistics, De La Salle University, 2401 Taft Avenue, Manila, 0922, Metro Manila, Philippines*

³*Max Planck Institute of Biochemistry, Am Klopferspitz 18, 82152, Martinsried near Munich, Germany*

⁴*Center for Complexity and Emerging Technologies, 2401 Taft Avenue, Manila, 0922, Metro Manila, Philippines*

Abstract

Several studies have developed dynamical models to understand the underlying mechanisms of insulin signaling, a signaling cascade that leads to the production of glucose - the human body's main source of energy. Reaction network analysis allows us to extract formal properties of dynamical systems without depending on their parameter values. This study focuses on the comparison of reaction network analysis of insulin signaling in healthy cell (INSMS or INSulin Metabolic Signaling) and in type 2 diabetes (INRES or INSulin RESistance). INSMS and INRES are similar with respect to some network, structo-kinetic, and kinetic properties. However, they differ in the following network properties: the networks have different species sets and functional modules, INRES is more complex than INSMS, and INRES loses the concordance of INSMS. Based on structo-kinetic properties, INSMS is injective while INRES is not. And one of the most significant differences between INSMS and INRES in terms of kinetic properties is the loss of ACR species in INRES (INSMS has 8 ACR species). These results show the insights we gain from analyzing kinetic realization, beyond what we already know from analyzing the dynamical systems of insulin signaling in healthy and insulin-resistant cells.

Keywords: insulin resistance, insulin signaling, kinetic realization, reaction network, sub-network

1 Introduction

Insulin signaling plays a crucial role in the human body's energy metabolism. Insulin reception triggers other processes that lead to the translocation of glucose, the body's main source of energy

*Corresponding author.

Emails: angelyn.lao@dlsu.edu.ph, pnlubenia@upd.edu.ph, eduardo.mendoza@dlsu.edu.ph

[32]. However, irregularities that decrease insulin reception can lead to insulin resistance in cells. Researchers have studied the role of insulin resistance in the development of many metabolic disorders such as type 2 diabetes, and of other phenomena in the human body including oxidative stress, inflammation, insulin receptor mutation, and mitochondrial dysfunction [20, 22, 29]. To this day, the underlying cause of insulin resistance has not been fully understood.

Mathematical models have helped the scientific community to better understand insulin signaling in healthy cells [14, 23, 24, 31] and diseased cells [1, 2, 21]. However, the complexity of metabolic insulin signaling have also naturally led to complicated dynamical models. The results generated from these models depend on simulations that rely on numerous parameter values that need to be identified from literature or derived from experimental data. Chemical Reaction Network Theory (CRNT) can address this challenge inherent in many dynamical systems.

CRNT translates a system of differential equations into a chemical reaction network (CRN) representation or kinetic realization of the system’s network of reactions. Constructing a particular kinetic realization of a system and identifying its kinetics allow the extraction of formal properties of the system, independent from parameter values of the model. Working with kinetic realizations also allows us to compare different instances of the same system, e.g., insulin signaling in healthy and insulin-resistant cells. One can also decompose the CRN representation into subnetworks to determine subgroups in the system, a task that is difficult to do with differential equations and biochemical maps. Several papers have taken advantage of the usefulness of CRNT in dealing with complex networks [10, 12, 17, 18, 30].

Formally, a CRN \mathcal{N} is a triple $(\mathcal{S}, \mathcal{C}, \mathcal{R})$ of nonempty finite sets $\mathcal{S} = \{X_1, \dots, X_m\}$, $\mathcal{C} = \{C_1, \dots, C_n\}$, and $\mathcal{R} = \{R_1, \dots, R_r\}$ of m species, n complexes, and r reactions, respectively. A complex appears as a reactant or a product in a reaction, and is a sum of species. After identifying a kinetics K (i.e., an assignment of rate functions to the reactions), we can then extract formal properties of the chemical kinetic system (\mathcal{N}, K) .

In this study, we use two systems of ordinary differential equations (ODEs): a model of insulin signaling in healthy cells by Sedaghat et al. [24] and a model of insulin signaling in type 2 diabetes by Nyman et al. [21]. Lubenia et al. [18] have constructed a kinetic realization of the Sedaghat et al. mass action model and have already performed a reaction network analysis of the system. Their key findings are as follows: (i) the underlying network is concordant; (ii) the network of three functional modules discussed by Sedaghat and colleagues form an independent decomposition; and (iii) the network has 8 species with absolute concentration robustness (ACR), one of which is the essential glucose transporter GLUT4 which, coupled with adequate glucose supply, enables reliable cellular energy production. We denote the kinetic realization of the insulin signaling in healthy cell by INSMS (INSulin Metabolic Signaling).

A natural next step is to check what happens to insulin signaling when there is insulin resistance. To this end, we use the Nyman et al. model of insulin signaling in type 2 diabetes. We then perform a comparative analysis of the kinetic realizations of the two states of insulin signaling, an analysis which, to our knowledge, is the first of its kind regarding metabolic insulin

signaling. Similar to the Sedaghat et al. model, the Nyman et al. model is also a mass action system, making our reaction network analysis parameter-free. We denote the kinetic realization of the insulin signaling in type 2 diabetes by INRES (INSulin RESistance).

In our comparative analysis, we look at the essential properties of INSMS and INRES. The properties considered are essential in the sense that they do not depend on the parameters, i.e., rate constants, used in the mass action models they were derived from. A network (or structural) property is one that can be specified in terms of the network components alone (e.g., concordance). Properties which may change under different dynamic equivalences are called structo-kinetic properties (e.g., monostationarity) while those which are invariant under any dynamic equivalence are called (purely) kinetic properties (e.g., ACR). This study confirms our expectation that kinetic system differences reveal interesting biological differences of the same system under differing states, i.e., healthy and insulin-resistant.

Both INSMS and INRES have subnetworks showing insulin receptor binding, IRS1 dynamics, and GLUT4 translocation. Both networks are also monostationary and all their positive equilibria are nondegenerate.

On the other hand, our main results show three major differences between the two models.

First, the (molecular) species involved in insulin signaling (and consequently the functional modules they constitute) differ strongly: out of 20 species in the healthy cell model, only 9 species occur among the 32 species in the insulin-resistant cell model. This and other properties point to a generally higher complexity of signal processing in the insulin-resistant case.

Second, INRES is discordant, i.e., the concordance of INSMS is lost. According to [28], concordant networks indicate “architectures that, by their very nature, enforce duller, more restrictive behavior despite what might be great intricacy in the interplay of many species, even independent of values that kinetic parameters might take”. This implies that there is a “less controlled” environment in an insulin-resistant cell.

Finally, there are no ACR species in INRES, marking the loss of ACR in 6 of its common species with INSMS, including the critical GLUT4 which is responsible for transporting glucose into the glycolytic system. The loss of ACR in GLUT4 implies that, in an insulin-resistant cell, the transporter becomes unreliable in cellular energy production.

The similarities and differences in the features of the two networks show that insulin signaling in healthy and insulin-resistant cells may start very similarly but eventually diverge, with the latter branching away from the former as a trigger occurs indicating that something is amiss with the system.

This paper is organized as follows: in Section 2, we summarize the results of the reaction network analysis of insulin signaling in healthy cells by [18]. In Section 3, we construct the kinetic realization of the model of insulin signaling in type 2 diabetes by [21]. Section 4 details the comparative analysis of network properties of INSMS and INRES while Section 5 considers the networks’ structo-kinetic and kinetic properties. Finally, we conclude the paper with a summary in Section 6. An Appendix with background on CRNT and other pertinent details of

the models considered is provided for the reader.

2 Reaction Network Analysis of Insulin Signaling in Healthy Cells

This section revisits the results of the reaction network analysis of Lubenia et al. [18] of a model of insulin signaling in healthy cells. They constructed a chemical reaction network (CRN) with mass action kinetics based on the insulin signaling model by Sedaghat et al. [24]. We denote this kinetic realization by INSMS (INSulin Metabolic Signaling). Tables 1 and 2 give the network numbers and an overview of the properties of INSMS. The reader may refer to Appendix A for a review of some basic concepts in Chemical Reaction Network Theory (CRNT).

Table 1: **Network numbers of INSMS** The high values of species, (reactant) complexes, reactions, (reactant) rank, and (reactant) deficiency quantify the high complexity of insulin signaling in healthy cells; the network numbers indicate that INSMS is a closed network with high reactant diversity; the network is also branching, t -minimal, not weakly reversible, and its terminal classes contain points and cycles.

Characteristic	Value
Species	20
Complexes	35
Reactant complexes	24
Reactions	35
Linkage classes	13
Strong linkage classes	24
Terminal strong linkage classes	13
Rank	15
Reactant rank	20
Deficiency	7
Reactant deficiency	4

INSMS is clearly a complex network as it involves 20 species, 35 complexes, and 35 reactions. It is a closed network with high reactant diversity. Viewed as a digraph, INSMS is branching, t -minimal, not (weakly) reversible, and its terminal classes contain points and cycles. Based on its stoichiometry, the network is positive dependent, of deficiency 7, nonconservative, and concordant. The authors also observed that INSMS has a nontrivial finest independent decomposition composed of 10 subnetworks. The biological significance of these and further properties are discussed in the succeeding chapters.

One of the key properties implied by the concordance of INSMS is its injectivity. The weak monotonicity of the mass action system implies that the network is also monostationary. Furthermore, all positive equilibria of INSMS are nondegenerate. And one of the most important

Table 2: **Overview of properties of INSMS** Some of the network properties listed are described in Table 1; INSMS has a positive equilibrium for some sets of rate constants (since it is positive dependent), its reactions have a high degree of linear dependence among each other (due to high deficiency), and is nonconservative and concordant; the key structo-kinetic properties of INSMS include its monostationarity (it cannot have multiple positive equilibria for a set of rate constants) and injectivity; its kinetic properties include the nondegeneracy of its equilibria and the existence of 8 ACR species in the system.

Property Class	INSMS	
Network	Closed	Not (weakly) reversible
	t -minimal	Branching
	Terminal classes include points and cycles	
	Positive dependent	Deficiency 7
	Nonconservative	Concordant
Structo-Kinetic	Monostationary	Injective
Kinetic	Nondegenerate equilibria	8 ACR species

results of Lubenia and colleagues was the discovery that 8 out of 20 species, including the critical GLUT4, in the insulin signaling in healthy cells has absolute concentration robustness (ACR).

3 Kinetic Realization of the Nyman et al. Model

In this section, we discuss the model of insulin signaling in type 2 diabetes by Nyman et al. [21]. After an overview of their biological findings, we construct a CRN representation of the dynamical system with mass action kinetics and discuss some of the basic properties of this kinetic realization.

3.1 Summary of Novel Biological Insights from the Model

Using data based on human adipocytes from healthy and diabetic individuals, Nyman and colleagues identified three hallmarks of insulin resistance in type 2 diabetes:

1. Diminished concentration of insulin receptors;
2. Low concentration of the glucose transporter GLUT4; and
3. Impaired feedback from mammalian target of rapamycin complex 1 (mTORC1) to insulin receptor substrate 1 (IRS1).

Remark 1. Hallmarks 1 and 2 are reflected in the loss of concentration robustness of the ACR species in INSMS (discussed in Section 5.5).

The model the authors used is a modification of an existing system of ordinary differential equations (ODEs) representing insulin signaling in type 2 diabetes constructed by Brännmark et

al. [2]. Nyman et al. added the extracellular signal-regulated kinase (ERK) signaling pathway, an important signaling branch in type 2 diabetes. After comparing observed data and generating simulations, the authors determined that, among the three main hallmarks of insulin resistance, the reduced positive feedback from mTORC1 to IRS1 could explain insulin resistance in all parts of the insulin signaling pathway.

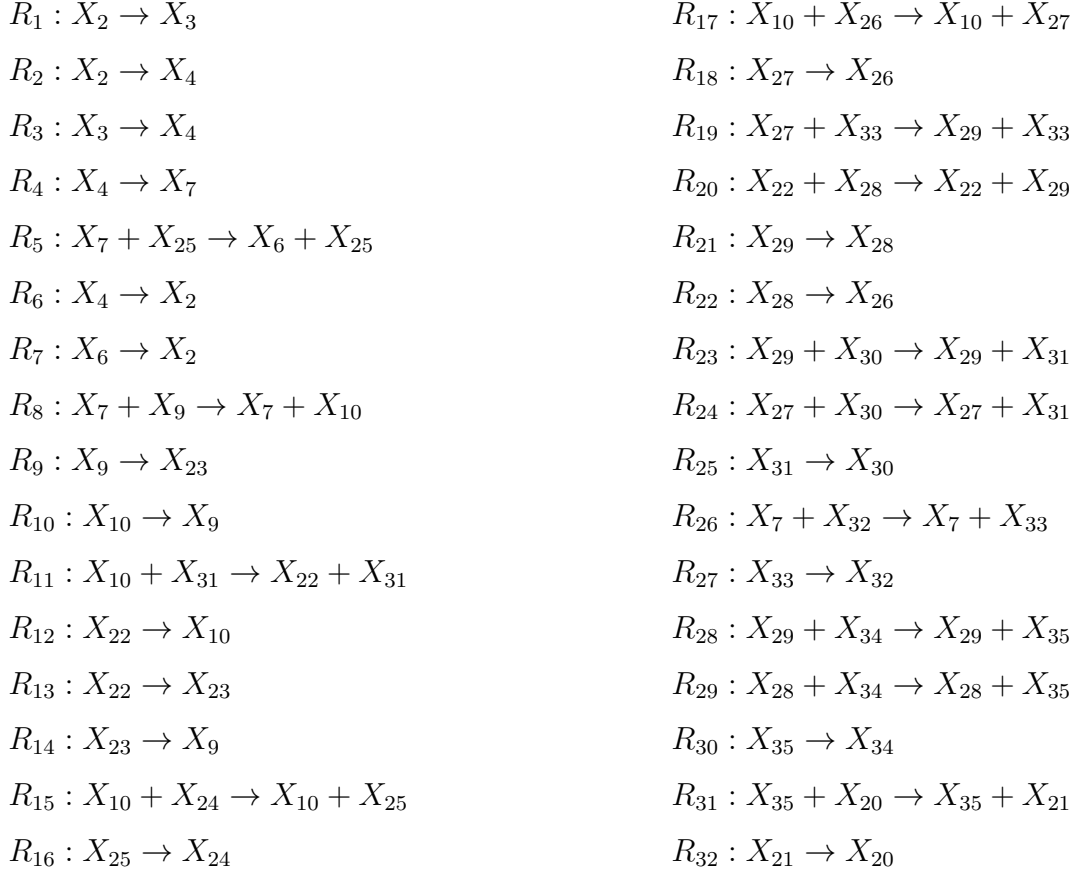
3.2 The Reaction Network of the Nyman et al. Model

The Nyman et al. model is composed of 32 ODEs (see Appendix B for the system of ODEs and the description of the variables). All 44 reactions in their model are modeled using mass action kinetics.

For easy comparison, the species occurring in both Sedaghat et al. and Nyman et al. models are denoted by the same variable. Variables for those occurring solely in Nyman et al.'s model continue their numbering from those in the Sedaghat et al. model.

For better visual orientation of the reader, we reconstruct the complete biochemical map of the Nyman et al. mass action system in Figure 1. The supplementary materials of Brännmark et al. [2] and Nyman et al. [21] contain details of the construction of the ODEs.

Applying the the Hars-Tóth criterion for mass action system realization as used in Lubenia et al. [18] and detailed in Chellaboina et al. [3], a kinetic realization of the Nyman et al. model is as follows:



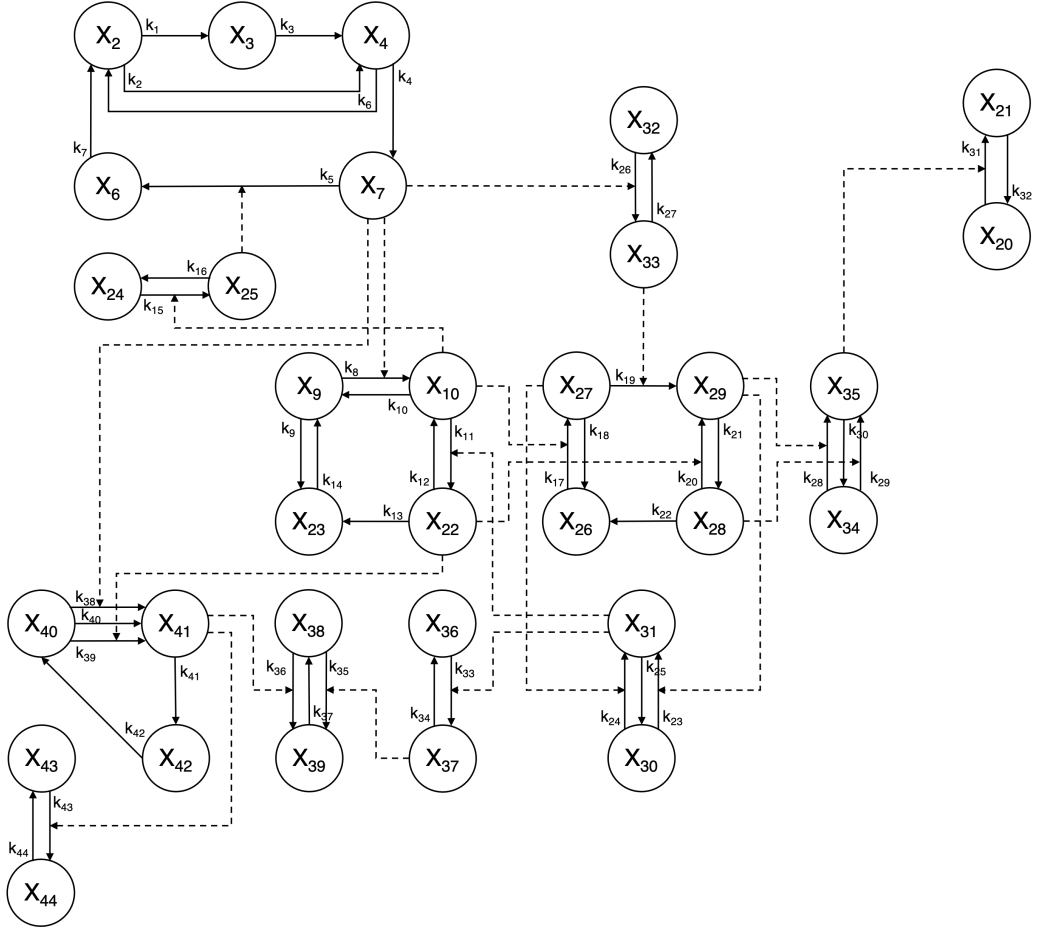
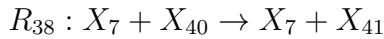
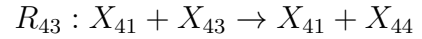
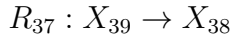
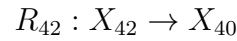
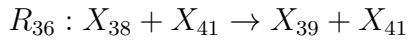
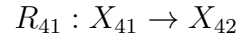
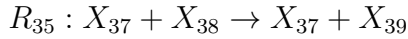
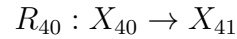
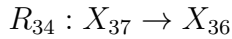
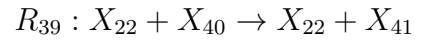
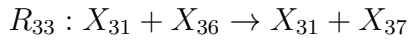


Figure 1: **Biochemical map of insulin signaling in type 2 diabetes** $X_2, X_3, X_4, X_6, X_7, X_9, X_{10}, X_{20}, \dots, X_{44}$ are the species of the network (see Appendix B for the description and units of the variables); k_1, \dots, k_{44} are the rate constants of the reactions; and solid lines represent mass transfer reactions while broken lines represent regulatory reactions; identifying subnetworks in insulin signaling in type 2 diabetes is difficult to do with biochemical maps but can be easily done using kinetic realizations



We denote this kinetic realization by INRES (INsulin RESistance) (also $\mathcal{N} = (\mathcal{S}, \mathcal{C}, \mathcal{R})$ with mass action kinetics K , set \mathcal{S} of 32 species, set \mathcal{C} of 70 complexes, and set \mathcal{R} of 44 reactions). Tables 3 and 4 present the network numbers and an overview of the properties of INRES.

The complexity of the network is evident in the network's high number of species, complexes, reactant complexes, and reactions, together with its high deficiency ($\delta = 19$). INRES is also a

Table 3: **Network numbers of INRES** The high values of species, (reactant) complexes, reactions, (reactant) rank, and (reactant) deficiency quantify the high complexity of insulin signaling in insulin-resistant cells; the network numbers indicate that INRES is a closed network ($s < m$) with high reactant diversity ($n_r > s$); the network is also branching ($r > n_r$), t -minimal ($t = \ell$), not weakly reversible ($s\ell \neq \ell$), and its terminal classes contain points ($t \neq n - n_r$) and cycles ($n \neq n_r$).

Characteristic	Notation	Value
Species	m	32
Complexes	n	70
Reactant complexes	n_r	41
Reactions	r	44
Linkage classes	ℓ	31
Strong linkage classes	$s\ell$	65
Terminal strong linkage classes	t	31
Rank	s	20
Reactant rank	q	32
Deficiency	δ	19
Reactant deficiency	δ_p	9

closed network (since $s = 20 < 32 = m$) with high reactant diversity (since $n_r = 41 > 20 = s$).

Viewed as a digraph, the network is not weakly reversible (since $s\ell = 65 \neq 31 = \ell$) but branching (since $r = 44 > 41 = n_r$). Other properties inferred by the numbers include its t -minimality (since $t = 31 = \ell$), and non-point terminality and non-cycle terminality (since $t \neq n - n_r = 29$ and $n - n_r \neq 0$, respectively).

Using the software CRNToolbox [7], we find that INRES is positive dependent, meaning there is a set of rate constants wherein the network has a positive equilibrium. The software’s Basic Report also indicates that the network is conservative. The Mass Action Injectivity Report shows that the system is not injective, implying that it is also discordant (this is confirmed by CRNToolbox’s Concordance Report). Finally, the Higher Deficiency Report concludes that INRES is monostationary, i.e., for a given set of rate constants, the network cannot admit multiple equilibria (moreover, an equilibrium of INRES cannot be degenerate).

3.3 The Finest Independent Decomposition

Applying the algorithm of Hernandez and De la Cruz [11], we find that the finest independent decomposition of

$\mathcal{N} = \{R_1, \dots, R_{44}\}$ (where R_1, \dots, R_{44} are the reactions of INRES) has 12 subnetworks:

$$\begin{aligned}
 \mathcal{N}_1 &= \{R_1, \dots, R_7\} & \mathcal{N}_4 &= \{R_{17}, \dots, R_{22}\} \\
 \mathcal{N}_2 &= \{R_8, \dots, R_{14}\} & \mathcal{N}_5 &= \{R_{23}, R_{24}, R_{25}\} \\
 \mathcal{N}_3 &= \{R_{15}, R_{16}\} & \mathcal{N}_6 &= \{R_{26}, R_{27}\}
 \end{aligned}$$

Table 4: **Overview of properties of INRES** Some of the network properties listed are described in Table 3; INRES has a positive equilibrium for some sets of rate constants (since it is positive dependent), its reactions have a high degree of linear dependence among each other (due to high deficiency), and is conservative and discordant; the key structo-kinetic properties of INRES include its monostationarity (it cannot have multiple positive equilibria for a set of rate constants) and non-injectivity; its kinetic properties include the nondegeneracy of its equilibria, and its lack of ACR species.

Property Class	INRES	
Network	Closed	Not (weakly) reversible
	t -minimal	Branching
	Terminal classes include points and cycles	
	Positive dependent	Deficiency 19
	Conservative	Discordant
Structo-Kinetic	Monostationary	Non-injective
Kinetic	Nondegenerate equilibria	No ACR species

$$\mathcal{N}_7 = \{R_{28}, R_{29}, R_{30}\}$$

$$\mathcal{N}_8 = \{R_{31}, R_{32}\}$$

$$\mathcal{N}_9 = \{R_{33}, R_{34}\}$$

$$\mathcal{N}_{10} = \{R_{35}, R_{36}, R_{37}\}$$

$$\mathcal{N}_{11} = \{R_{38}, \dots, R_{42}\}$$

$$\mathcal{N}_{12} = \{R_{43}, R_{44}\}.$$

Table 5 presents the network numbers of the subnetworks of INRES. The analysis and biological implications of the decomposition are discussed in Section 4.2.

4 Comparative Analysis of Network Properties of INSMS and INRES

This section compares the network properties of INSMS and INRES. A **network property** is one that can be specified in terms of the network components alone, i.e., there is no need for specifying a kinetics.

We highlight three differing network properties:

1. The sets of species (consequently, functional modules) of the networks are different;
2. There is a much higher level of complexity in INRES; and
3. The concordance of INSMS is lost, i.e., INRES is discordant.

We conclude the section with a discussion of further differences between the network properties of the two kinetic realizations.

Table 5: **Network numbers of the subnetworks of INRES** The finest independent decomposition of INRES has 12 subnetworks representing different processes involved in insulin signaling in type 2 diabetes

Characteristics	\mathcal{N}_1	\mathcal{N}_2	\mathcal{N}_3	\mathcal{N}_4	\mathcal{N}_5	\mathcal{N}_6	\mathcal{N}_7	\mathcal{N}_8	\mathcal{N}_9	\mathcal{N}_{10}	\mathcal{N}_{11}	\mathcal{N}_{12}
Species	6	6	3	7	4	3	4	3	3	4	5	3
Complexes	7	8	4	10	6	4	6	4	4	6	7	4
Reactant complexes	5	6	2	6	3	2	3	2	2	3	5	2
Reactions	7	7	2	6	3	2	3	2	2	3	5	2
Linkage classes	2	3	2	4	3	2	3	2	2	3	3	2
Strong linkage classes	5	7	4	10	6	4	6	4	4	6	5	4
Terminal strong linkage classes	2	3	2	4	3	2	3	2	2	3	3	2
Rank	4	3	1	3	1	1	1	1	1	1	2	1
Reactant rank	5	6	2	6	3	2	3	2	2	3	5	2
Deficiency	1	2	1	3	2	1	2	1	1	2	2	1
Reactant deficiency	0	0	0	0	0	0	0	0	0	0	0	0

4.1 Common Network Properties

Comparing Tables 2 and 4, we observe that INSMS and INRES are both branching, t -minimal, positive dependent, not (weakly) reversible, non-point terminal, and non-cycle terminal. Based on Sections 2 and 3.2, both are also closed networks with high reactant diversity.

Lemma 3.5.4 of Feinberg [6] and Proposition 1 of Lubenia et al. [18] show that a positive dependent network has a set of rate constants such that the corresponding mass action system has a positive equilibrium. This result is important when we check INRES for ACR species in Section 5.5.

4.2 Differences in Species Sets and Functional Modules

Among the 20 species in INSMS, only nine appear in INRES as well. Seven of these are involved in the initial signaling steps while the other two are significant in the process of glucose transfer to the glycolytic system. There are 23 unique species in INRES (i.e., those not in INSMS). This difference in species sets clearly shows that the functional modules active in the intermediate steps of the two networks are entirely different, suggesting a “forking” of the process based on the reduced amount of glucose available for energy production.

Lubenia et al.’s reaction network analysis of INSMS revealed the three functional modules used by Sedaghat et al. in the construction of their model. A coarsening of the finest independent decomposition of INRES also shows these functional modules. A **coarsening** of a decomposition has some of the original subnetworks combined to form fewer subnetworks. Thus, a coarsening of INRES can show the functional modules involved in insulin signaling in type 2 diabetes.

Consider the coarsening described in Table 6. \mathcal{N}_1^* , \mathcal{N}_2^* , and \mathcal{N}_3^* correspond to the subsystems used to construct the Sedaghat et al. model (insulin receptor binding and recycling,

postreceptor signaling, and GLUT4 translocation, respectively), albeit with different actors. The last subnetwork \mathcal{N}_4^* appears in the Nyman et al. model only; it is a signaling branch (composed of S6 and S6K formation from mTORC, ERK signaling pathway, and nuclear transcription) that the authors deemed significant in insulin signaling in type 2 diabetes.

Table 6: **Coarsening of the finest independent decomposition of INRES in relation to the Sedaghat et al. model** \mathcal{N}_1^* , \mathcal{N}_2^* , and \mathcal{N}_3^* correspond to the insulin receptor binding and recycling subsystem, postreceptor signaling subsystem, and GLUT4 translocation subsystem, respectively; \mathcal{N}_4^* is a subsystem found in the Nyman et al. model representing a signaling branch (composed of S6 and S6K formation from mTORC, ERK signaling pathway, and nuclear transcription) that the authors deemed significant in insulin signaling in type 2 diabetes.

$$\mathcal{N} = \mathcal{N}_1^* \cup \mathcal{N}_2^* \cup \mathcal{N}_3^* \cup \mathcal{N}_4^*$$

\mathcal{N}_1^*	\mathcal{N}_1
\mathcal{N}_2^*	$\mathcal{N}_2 \cup \dots \cup \mathcal{N}_6$
\mathcal{N}_3^*	$\mathcal{N}_7 \cup \mathcal{N}_8$
\mathcal{N}_4^*	$\mathcal{N}_9 \cup \dots \cup \mathcal{N}_{12}$

Table 7 presents another coarsening of the 12 subnetworks of INRES which reveals the 9 subsystems that Nyman and colleagues considered in the construction of their model. Subsystems \mathcal{N}'_1 to \mathcal{N}'_9 correspond to the insulin receptor signaling, IRS1 dynamics, negative feedback to insulin receptors, PBK dynamics, mTORC dynamics, GLUT4 translocation, S6 and S6K formation from mTORC, ERK signaling pathway, and nuclear transcription, respectively.

Table 7: **Coarsening of the finest independent decomposition of INRES in relation to the Nyman et al. model** \mathcal{N}'_1 to \mathcal{N}'_9 correspond to the insulin receptor signaling, IRS1 dynamics, negative feedback to insulin receptors, PBK dynamics, mTORC dynamics, GLUT4 translocation, S6 and S6K formation from mTORC, ERK signaling pathway, and nuclear transcription, respectively.

$$\mathcal{N} = \mathcal{N}'_1 \cup \mathcal{N}'_2 \cup \mathcal{N}'_3 \cup \mathcal{N}'_4 \cup \mathcal{N}'_5 \cup \mathcal{N}'_6 \cup \mathcal{N}'_7 \cup \mathcal{N}'_8 \cup \mathcal{N}'_9$$

\mathcal{N}'_1	\mathcal{N}_1
\mathcal{N}'_2	\mathcal{N}_2
\mathcal{N}'_3	\mathcal{N}_3
\mathcal{N}'_4	\mathcal{N}_4
\mathcal{N}'_5	$\mathcal{N}_5 \cup \mathcal{N}_6$
\mathcal{N}'_6	$\mathcal{N}_7 \cup \mathcal{N}_8$
\mathcal{N}'_7	$\mathcal{N}_9 \cup \mathcal{N}_{10}$
\mathcal{N}'_8	\mathcal{N}_{11}
\mathcal{N}'_9	\mathcal{N}_{12}

In the finest independent decomposition of INRES, subnetwork \mathcal{N}'_2 is significant because it contains reaction R_{11} which exhibits the mTORC feedback to IRS1. Affecting this feedback are reactions R_{23} and R_{24} in subnetwork \mathcal{N}'_5 : these are the reactions for the activation of mTORC.

These reactions together form the “single mechanism” that explains insulin resistance in type 2 diabetes according to Nyman et al.: an attenuated positive feedback from mTORC to IRS1.

Aside from the number of species and functional modules, the number of reactions and the value of the deficiency of INRES also indicate that it is more complex than INSMS. Although INRES has only nine more reactions (44 vs 35), its deficiency is nearly triple that of INSMS (19 vs 7), signifying a much higher level of (linear) dependence among the reactions. On the other hand, the reactant deficiency more than doubles “only” from 4 to 9. This appears to be mainly due to the (maximally) high reactant rank of INRES (32 vs 20 for INSMS). The length of the finest independent decomposition of INRES (12 vs 10 for INSMS) gives further testament to its higher complexity compared to INSMS. Although this difference is relatively moderate, this is consistent with the rank relation (20 for INRES vs 15 for INSMS).

4.3 Concordance vs Discordance

The most significant difference between INSMS and INRES in terms of network properties is the concordance of the former and the discordance of the latter. Discordance marks the loss of a network characteristic which Shinar and Feinberg consider to indicate “architectures that, by their very nature, enforce duller, more restrictive behavior despite what might be great intricacy in the interplay of many species, even independent of values that kinetic parameters might take” [28]. The discordance of INRES is potentially related to the “forking” in insulin signaling in healthy cells and type 2 diabetes mentioned in Section 4.2. The root causes of discordance will be discussed in Section 5.2.

Remark 2. While large classes of biochemical systems have been shown to be discordant, only a handful of systems have been published as having the concordance property. For example, Fariñas et al. [4] have shown that the independent kinetic realization of any S-system in two or more variables is discordant. To our knowledge, only three concordant biochemical networks have been published to date: a kinetic realization of the Wnt signaling pathway in Chapter 10.5.4 of Feinberg [6], of the insulin signaling in healthy cells by Lubenia et al. [18], and of the Schmitz carbon cycle model by Fortun and Mendoza [10].

4.4 Further Differences in Network Properties

Table 8 provides an overview of further differences between INSMS and INRES.

The analysis of Lubenia et al. showed that INSMS is nonconservative while CRNToolbox results reveal that INRES is conservative. The nonconservativity of INSMS was a necessary condition for the ACR in 8 species in INSMS to be inferred from ACR in its deficiency zero subnetwork. Meanwhile, INRES has no deficiency zero subnetwork and, as will be shown in Section 5.5, has no ACR species as well.

Lubenia et al. also observed that INSMS has nine (out of 10) subnetworks whose rank is 1. In INRES, eight (out of 12) subnetworks have rank 1. The Meshkat et al. criterion [19] was

Table 8: **Further differences between INSMS and INRES** The nonconservativity of INSMS, and its deficiency zero subnetworks and rank 1 subnetworks are significant in the existence of ACR species in the network; INRES, on the other hand, is conservative and, as shown in Section 5.5, has no ACR species.

INSMS	INRES	Comment
Nonconservative	Conservative	
5 (of 10) subnetworks with $\delta = 0$	0 (of 12) subnetworks with $\delta = 0$	Large subnetwork ($s = 10$) with $\delta = 0$ in INSMS
9 (of 10) subnetworks with $s = 1$	8 (of 12) subnetworks with $s = 1$	
0 (of 10) subnetworks with $\delta_\rho = 0$	12 (of 12) subnetworks with $\delta_\rho = 0$	Each subnetwork has reactant set linear independent kinetics in INRES

applied to the INSMS rank 1 subnetworks to determine two ACR species. We tried applying the said criterion to rank 1 subnetworks of INRES to determine ACR species but the effort yielded no results.

Finally, another difference between INSMS and INRES is terms of the number of subnetworks with zero reactant deficiency: INSMS has none while every subnetwork of INRES has a reactant deficiency of zero.

5 Comparative Analysis of Structo-kinetic and Kinetic Properties of INSMS and INRES

In this section, we discuss the structo-kinetic and kinetic properties of INSMS and INRES, and explore their relationships to insulin signaling in healthy and insulin-resistant cells. **Structo-kinetic properties** are properties that depend on both network and kinetic properties while **(purely) kinetic properties** depend on the kinetics alone.

We also highlight in this section the most striking difference in kinetic properties of the two networks: INSMS has 8 ACR species while INRES has none.

5.1 Common Structo-kinetic Properties

The first common structo-kinetic property of INSMS and INRES is the absence of complex balanced equilibria since both networks are not weakly reversible.

Secondly, the t -minimality of both networks implies the coincidence of their respective kinetic and stoichiometric subspaces [8].

An interesting third structo-kinetic commonality of INSMS and INRES is their monostationarity for any mass action kinetics: the network cannot admit multiple positive equilibria for a given a set of rate constants. For INSMS, this property derives from a general property of weakly

monotonic kinetics on a concordant network. For INRES, monostationarity was concluded by the Higher Deficiency Report of CRNToolbox and is considered an infrequent phenomenon in view of the underlying network’s discordance.

5.2 Injective vs Non-injective

The reaction network analysis of INSMS showed that it is injective since the network is concordant. On the other hand, the non-injectivity of INRES is shown by the Mass Action Injectivity Report of the CRNToolbox.

Based on Theorem 4.11 of Shinar and Feinberg, the class of concordant networks is precisely the class of networks that are injective for every assignment of a weakly monotonic kinetics [27]. Since every mass action kinetics is weakly monotonic, the root cause of the discordance of INRES is the combination of two factors: the weak monotonicity and non-injectivity of its kinetics.

5.3 Monostationarity in All Weakly Monotonic Systems vs Multistationarity for Some Weakly Monotonic Systems

Sections 5.1 and 5.2 show that while the injectivity of INSMS, induced by a weakly monotonic kinetics on a concordant network, is lost on the discordant INRES, monostationarity is maintained.

Since INSMS is a concordant network, then it has injectivity in all weakly monotonic kinetic systems derived from it (Theorem 4.11 of Shinar and Feinberg [27]). Moreover, together with Remark 4.4 in Shinar and Feinberg [27], we conclude that INSMS is monostationary in all weakly monotonic systems.

Despite its monostationarity for any mass action kinetics, it follows from Theorem 10.5.10 of [6] that for some weakly monotonic kinetics, INRES will have the capacity for multiple positive equilibria in a stoichiometric class, i.e., the network can display multistationarity. The root of this is, hence, the network property of discordance in combination with the weak monotonicity of its kinetics.

5.4 Common Kinetic Properties

We observed only a single common kinetic property of INSMS and INRES: the non-degeneracy of all their positive equilibria. This property can be derived from the t -minimality of both networks: t -minimality is a necessary condition for the existence of nondegenerate equilibria, as detailed in Remark 4.11 of Feinberg and Horn [8].

Remark 3.

1. This kinetic property also implies the common structo-kinetic property of coincidence of the kinetic and stoichiometric subsets.

2. The nondegeneracy of all equilibria of INSMS was a consequence of concordance of the underlying network: if a concordant network has weakly monotonic kinetics, then all equilibria are degenerate. On the other hand, for INRES, the nondegeneracy of its equilibria came from CRNToolbox results.

5.5 Presence of ACR in 8 of 20 Species vs. Absence of ACR in 32 Species

ACR is the invariance of the concentrations of a species at all positive equilibria of a kinetic system [25, 26]. In Section 4.1, we showed that INSMS and INRES have a positive equilibrium for a set of rate constants. Thus, we can check for ACR species in both networks. Lubenia and colleagues already showed that INSMS has 8 species (out of 20) with ACR and it is noteworthy that this set of species includes GLUT4, the glucose transporter essential for feeding the glycolytic process with glucose. ACR of a species implies that the species is reliable in maintaining the efficiency of the process it belongs to.

Applying the algorithm of Fortun et al. [9] and the Meshkat et al. criterion [19], we find that, remarkably, none of the 32 species in INRES have ACR. Significantly, GLUT4 lost its concentration robustness, indicating that it lost its reliability in sustaining efficient energy production in an insulin-resistant cell.

Remark 4. Aside from GLUT4, five of the other species from INSMS, which lost their ACR in INRES, are pooled insulin receptors. Hence, the first two key biological findings of Nyman et al. on lower concentration of receptors and GLUT4 (see Section 3.1) are also reflected in the loss of ACR.

5.5.1 Equilibria Parametrization Method Applied to the Sedaghat et al. Model

Hernandez et al. [12] developed a method to determine the parameterized equilibrium of a mass action system. They did this using the fact that the set of positive equilibria of the whole network is the intersection of the equilibria sets of the subnetworks [5], together with network translation methods developed by Johnston and colleagues [15, 16].

The analysis of INSMS showed that the number of ACR species $m_{\text{ACR}} \geq 8$ for all rate constants and $m_{\text{ACR}} = 8$ for some. Subsequently, Hernandez et al. [12] sharpened this to $m_{\text{ACR}} = 8$ for all rate constants using their method applied to the Sedaghat et al. model.

5.5.2 Equilibria Parametrization Method Applied to the Nyman et al. Model

To verify that INRES indeed has no ACR species, we tried using the Hernandez et al. method to derive the parametrized equilibrium of the Nyman et al. model. However, since their method did not deliver full results, we used network decomposition to compute manually the equilibria relationships and obtained the following solution:

$$\begin{aligned}
X_2 &= \frac{k_3}{k_1} X_3 \\
X_4 &= \frac{k_3(k_2 + k_1)}{k_1(k_4 + k_6)} X_3 \\
X_6 &= \frac{k_4 k_3 (k_2 + k_1)}{k_7 k_1 (k_4 + k_6)} X_3 \\
X_9 &= \left(\frac{k_{10}}{k_8} + \frac{k_{13} k_{11}}{k_8 (k_{12} + k_{13})} X_{31} \right) \frac{X_{10}}{X_7} \\
X_{20} &= \frac{k_{32}}{\left(1 + \frac{k_{20} k_{11}}{k_{22} (k_{12} + k_{13})} X_{10} X_{31} \right) \frac{k_{31} k_{28} k_{19} k_{17}}{k_{30} k_{21} (k_{18} + k_{19} X_{33})} X_{10} X_{26} X_{33} X_{34} + \frac{k_{31} k_{29} k_{19} k_{17}}{k_{30} k_{22} (k_{18} + k_{19} X_{33})} X_{10} X_{26} X_{33} X_{34}} X_{21} \\
X_{22} &= \frac{k_{11}}{k_{12} + k_{13}} X_{10} X_{31} \\
X_{23} &= \frac{k_9 k_{10}}{k_{14} k_8} \frac{X_{10}}{X_7} + \left(\frac{k_9}{k_8} \frac{1}{X_7} + 1 \right) \frac{k_{13} k_{11}}{k_{14} (k_{12} + k_{13})} X_{10} X_{31} \\
X_{24} &= \frac{k_{16} k_4 k_3 (k_2 + k_1)}{k_{15} k_5 k_1 (k_4 + k_6)} \frac{X_3}{X_7 X_{10}} \\
X_{25} &= \frac{k_4 k_3 (k_2 + k_1)}{k_5 k_1 (k_4 + k_6)} \frac{X_3}{X_7} \\
X_{27} &= \frac{k_{17}}{k_{18} + k_{19} X_{33}} X_{10} X_{26} \\
X_{28} &= \frac{k_{19} k_{17}}{k_{22} (k_{18} + k_{19} X_{33})} X_{10} X_{26} X_{33} \\
X_{29} &= \left(1 + \frac{k_{20} k_{11}}{k_{22} (k_{12} + k_{13})} X_{10} X_{31} \right) \frac{k_{19} k_{17}}{k_{21} (k_{18} + k_{19} X_{33})} X_{10} X_{26} X_{33} \\
X_{30} &= \frac{k_{25}}{\left(1 + \frac{k_{20} k_{11}}{k_{22} (k_{12} + k_{13})} X_{10} X_{31} \right) \frac{k_{23} k_{19} k_{17}}{k_{21} (k_{18} + k_{19} X_{33})} X_{10} X_{26} X_{33} + \frac{k_{24} k_{17}}{k_{18} + k_{19} X_{33}} X_{10} X_{26}} X_{31} \\
X_{32} &= \frac{k_{27}}{k_{26}} \frac{X_{33}}{X_7} \\
X_{35} &= \left(1 + \frac{k_{20} k_{11}}{k_{22} (k_{12} + k_{13})} X_{10} X_{31} \right) \frac{k_{28} k_{19} k_{17}}{k_{30} k_{21} (k_{18} + k_{19} X_{33})} X_{10} X_{26} X_{33} X_{34} \\
&\quad + \frac{k_{29} k_{19} k_{17}}{k_{30} k_{22} (k_{18} + k_{19} X_{33})} X_{10} X_{26} X_{33} X_{34} \\
X_{37} &= \frac{k_{33}}{k_{34}} X_{31} X_{36} \\
X_{39} &= \frac{k_{35} k_{33}}{k_{37} k_{34}} X_{31} X_{36} X_{38} + \frac{k_{36}}{k_{37}} X_{38} X_{41} \\
X_{40} &= \frac{k_{41}}{k_{38} X_7 + \frac{k_{39} k_{11}}{k_{12} + k_{13}} X_{10} X_{31} + k_{40}} X_{41} \\
X_{42} &= \frac{k_{41}}{k_{42}} X_{41} \\
X_{44} &= \frac{k_{43}}{k_{44}} X_{41} X_{43}
\end{aligned}$$

Observe that the parametrized equilibrium of the species above depend on X_3 , X_7 , X_{10} , X_{21} , X_{26} , X_{31} , X_{33} , X_{34} , X_{36} , X_{38} , X_{41} , and X_{43} , implying that there are infinitely many possible equilibrium solutions for the system. We, therefore, conclude that INRES has no ACR species.

6 Summary and Conclusion

To study and understand the underlying mechanism of insulin signaling, we have constructed, analyzed, and compared INSMS and INRES. In [18], we performed a reaction network analysis on a kinetic realization of a model of metabolic insulin signaling in healthy cells (INSMS). For the convenience of the reader, we have provided a summary of the results in Section 2. In Section 3, we constructed a CRN of a model of insulin signaling in an insulin-resistant cell (INRES).

We then compared the different network, structo-kinetic, and kinetic properties of the two reaction networks. We have summarized in a table in Appendix C all the properties of INSMS and INRES discussed in this paper. We observed that INSMS and INRES are both closed, positive dependent, and branching networks with high reactant diversity. They are also t -minimal, and their terminal classes contain points and cycles. Both networks are monostationary, with all their equilibria being nondegenerate, but they have no complex balanced equilibria. Three main network properties are different between INSMS and INRES: they have very different sets of species (consequently, their functional modules are dissimilar as well); INRES has a much higher level of complexity than INSMS; and the concordance of INSMS is lost in INRES.

In terms of structo-kinetic properties, INSMS is an injective network while INRES is non-injective. We also observed that INSMS is monostationary in all weakly monotonic systems while INRES may have the capacity for multistationarity for some weakly monotonic systems. One of the most important differences between INSMS and INRES is the kinetic property of ACR: INSMS has 8 ACR species while INRES has none.

These findings, from our view, have shown the usefulness of doing a kinetic realization, beyond what we already know from the analysis of the dynamical systems of Sedaghat et al. and Nyman et al.

References

- [1] Braatz, E, Coleman, R (2015) A mathematical model of insulin resistance in Parkinson's disease. *Comput Biol Chem* 56:84–97.
<https://doi.org/10.1016/j.compbiolchem.2015.04.003>
- [2] Brännmark C, Nyman E, Fagerholm S, Bergenholm L, Ekstrand E, Cedersund G, Strålfors P (2013) Insulin signaling in type 2 diabetes: experimental and modeling analyses reveal mechanisms of insulin resistance in human adipocytes. *J Biol Chem* 288(14):9867–9880.
<https://doi.org/10.1074/jbc.m112.432062>

- [3] Chellaboina V, Bhat S, Haddad W, Bernstein D (2009) Modeling and analysis of mass-action kinetics. *IEEE Control Syst* 29(4):60–78. <https://doi.org/10.1109/MCS.2009.932926>
- [4] Fariñas H, Mendoza E, Lao A (2021) Chemical reaction network decompositions and realizations of S-systems. *Philipp Sci Lett* 14(1):147–157
- [5] Feinberg M (1987) Chemical reaction network structure and the stability of complex isothermal reactors: I. The deficiency zero and deficiency one theorems. *Chem Eng Sci* 42(10):2229–2268. [https://doi.org/10.1016/0009-2509\(87\)80099-4](https://doi.org/10.1016/0009-2509(87)80099-4)
- [6] Feinberg M (2019) *Foundations of chemical reaction network theory*. Springer, Switzerland, <https://doi.org/10.1007/978-3-030-03858-8>
- [7] Feinberg M, Ellison P, Ji H, Knight D (2018) *The Chemical Reaction Network Toolbox Version 2.35*. <https://doi.org/10.5281/zenodo.5149266>
- [8] Feinberg M, Horn J (1977) Chemical mechanism structure and the coincidence of the stoichiometric and kinetic subspaces. *Arch Ration Mech Anal* 66(1):83–97. <https://doi.org/10.1007/bf00250853>
- [9] Fontanil L, Mendoza E, Fortun N (2021) A computational approach to concentration robustness in power law kinetic systems of Shinar-Feinberg type. *MATCH Commun Math Comput Chem* 86(3):489–516
- [10] Fortun N, Mendoza E (2023) Comparative analysis of carbon cycle models via kinetic representations. *J Math Chem* 61:896–932. <https://doi.org/10.1007/s10910-022-01442-8>
- [11] Hernandez B, De la Cruz R (2021) Independent decompositions of chemical reaction networks. *Bull Math Biol* 83(76):1–23. <https://doi.org/10.1007/s11538-021-00906-3>
- [12] Hernandez B, Lubenia P, Johnston M, Kim J (2023) A framework for deriving analytic steady states of biochemical reaction networks. *PLoS Comput Biol* 19(4):e1011039. <https://doi.org/10.1371/journal.pcbi.1011039>
- [13] Hernandez B, Mendoza E (2021) Positive equilibria of Hill-type kinetic systems. *J Math Chem* 59:840–870. <https://doi.org/10.1007/s10910-021-01230-w>
- [14] Huang C, Wu M, Du J, Liu D, Chan C (2014) Systematic modeling for the insulin signaling network mediated by IRS1 and IRS2. *J Theor Biol* 355:40–52. <https://doi.org/10.1016/j.jtbi.2014.03.030>
- [15] Johnston M, Burton E (2019) Computing weakly reversible deficiency zero network translations using elementary flux modes. *Bull Math Biol* 81:1613–1644. <https://doi.org/10.1007/s11538-019-00579-z>

- [16] Johnston M, Müller S, Pantea C (2019) A deficiency-based approach to parameterizing positive equilibria of biochemical reaction systems. *Bull Math Biol* 81:1143–1172. <https://doi.org/10.1007/s11538-018-00562-0>
- [17] Karp R, Pérez-Millán M, Dasgupta T, Dickenstein A, Gunawardena J (2012) Complex-linear invariants of biochemical networks. *J Theor Biol* 311:130–138. <https://doi.org/10.1016/j.jtbi.2012.07.004>
- [18] Lubenia P, Mendoza E, Lao A (2022) Reaction network analysis of metabolic insulin signaling. *Bull Math Biol* 84(129):1–22. <https://doi.org/10.1007/s11538-022-01087-3>
- [19] Meshkat N, Shiu A, Torres A (2022) Absolute concentration robustness in networks with low-dimensional stoichiometric subspace. *Vietnam J Math* <https://doi.org/10.1007/s10013-021-00524-5>
- [20] Nguyen T, Ta Q, Nguyen T, Le T, Vo V (2020) Role of insulin resistance in the Alzheimer’s disease progression. *Neurochem Res* 45:1481–1491. <https://doi.org/10.1007/s11064-020-03031-0>
- [21] Nyman E, Rajan M, Fagerholm S, Brännmark C, Cedersund G, Strålfors P (2014) A single mechanism can explain network-wide insulin resistance in adipocytes from obese patients with type 2 diabetes. *J Biol Chem* 289(48):33215–33230. <https://doi.org/10.1074/jbc.M114.608927>
- [22] Ormazabal V, Nair S, Elfeky O, Aguayo C, Salomon C, Zuñiga F (2018) Association between insulin resistance and the development of cardiovascular disease. *Cardiovasc Diabetol* 17:1–14. <https://doi.org/10.1186/s12933-018-0762-4>
- [23] Quon, Michael J. and Campfield, L. Arthur (1991) A mathematical model and computer simulation study of insulin receptor regulation. *J Theor Biol* 150(1):59–72. [https://doi.org/10.1016/S0022-5193\(05\)80475-8](https://doi.org/10.1016/S0022-5193(05)80475-8)
- [24] Sedaghat A, Sherman A, Quon M (2002) A mathematical model of metabolic insulin signaling pathways. *Am J Physiol Endocrinol Metab* 283(5):E1084–E1101. <https://doi.org/10.1152/ajpendo.00571.2001>
- [25] Shinar G, Feinberg M (2010) Structural sources of robustness in biochemical reaction networks. *Science* 327(5971):1389–1391. <https://doi.org/10.1126/science.1183372>
- [26] Shinar G, Feinberg M (2011) Design principles for robust biochemical reaction networks: What works, what cannot work, and what might almost work. *Math Biosci* 231(1):39–48. <https://doi.org/10.1016/j.mbs.2011.02.012>

- [27] Shinar G, Feinberg M (2012) Concordant chemical reaction networks. *Math Biosci* 240(2):92–113. <https://doi.org/10.1016/j.mbs.2012.05.004>
- [28] Shinar G, Feinberg M (2013) Concordant chemical reaction networks and the species-reaction graph. *Math Biosci* 241(1):1–23. <https://doi.org/10.1016/j.mbs.2012.08.002>
- [29] Tanase D, Gosav E, Costea C, Ciocoiu M, Lacatusu C, Maranduca M, Ouatu A, Floria M (2020) The intricate relationship between type 2 diabetes mellitus (T2DM), insulin resistance (IR), and nonalcoholic fatty liver disease (NAFLD). *J Diabetes Res* 2020:1–16. <https://doi.org/10.1155/2020/3920196>
- [30] Villar J, Lubenia P, Mendoza E, Arceo C (2019) Structural stability analysis of models of dopamine synthesis and D1 receptor trafficking in RPT cells using CRNT. *Philipp J Sci* 148(3):523–533
- [31] Wanant S, Quon M (2000) Insulin receptor binding kinetics: Modeling and simulation studies. *J Theor Biol* 205(3):355–364. <https://doi.org/10.1006/jtbi.2000.2069>
- [32] Yaribeygi H, Farrokhi F, Butler A, Sahebkar A (2019) Insulin resistance: Review of the underlying molecular mechanisms. *J Cell Physiol* 234(6):8152–8161. <https://doi.org/10.1002/jcp.27603>

Appendix A Notations and Definition of Terms

In this section, we lay the foundation of Chemical Reaction Network Theory by discussing the definition of terms used in the paper. After discussing the fundamentals of chemical reaction networks and kinetic systems, we review important terminologies related to decomposition theory.

A.1 Chemical Reaction Networks

A **chemical reaction network** (CRN) \mathcal{N} is a triple $(\mathcal{S}, \mathcal{C}, \mathcal{R})$ of nonempty finite sets \mathcal{S} , \mathcal{C} , and \mathcal{R} of m species, n complexes, and r reactions, respectively, where $\mathcal{C} \subseteq \mathbb{R}_{\geq 0}^{\mathcal{S}}$ and $\mathcal{R} \subset \mathcal{C} \times \mathcal{C}$ satisfying the following:

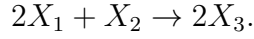
(i) $(C, C) \notin \mathcal{R}$ for any $C \in \mathcal{C}$; and

(ii) For each $C_i \in \mathcal{C}$, there exists $C_j \in \mathcal{C}$ such that $(C_i, C_j) \in \mathcal{R}$ or $(C_j, C_i) \in \mathcal{R}$.

Given a set I , \mathbb{R}^I refers to the vector space of real-valued functions with domain I . If x is a vector in \mathbb{R}^I , we use the symbol x_i to denote the number that x assigns to $i \in I$. In the context of a CRN, $\mathbb{R}^{\mathcal{S}}$, $\mathbb{R}^{\mathcal{C}}$, and $\mathbb{R}^{\mathcal{R}}$ are referred to as the **species space**, **complex space**, and **reaction space**, respectively.

In a CRN, we denote the species as X_1, \dots, X_m . This way, X_i can be identified with the vector in \mathbb{R}^m with 1 in the i th coordinate and zero elsewhere. We denote the reactions as R_1, \dots, R_r . We denote the complexes as C_1, \dots, C_n where the manner in which the complexes are numbered play no essential role. A complex $C_i \in \mathcal{C}$ is given as $C_i = \sum_{j=1}^m c_{ij} X_j$ or as the vector $(c_{i1}, \dots, c_{im}) \in \mathbb{R}^m$. The coefficient c_{ij} is called the **stoichiometric coefficient** of species X_j in complex C_i . Stoichiometric coefficients are all nonnegative numbers. We define the **zero complex** as the zero vector in \mathbb{R}^m . The ordered pair (C_i, C_j) corresponds to the familiar notation $C_i \rightarrow C_j$ which indicates the reaction where complex C_i reacts to complex C_j . We call C_i the **reactant complex** and C_j the **product complex**. We denote the number of reactant complexes as n_r .

Example A.1. Consider the reaction



X_1, X_2 , and X_3 are the species, the reactant complex is $2X_1 + X_2$, and $2X_3$ is the product complex. The stoichiometric coefficients are 2, 1, and 2 for X_1, X_2 , and X_3 , respectively.

Let $\mathcal{N} = (\mathcal{S}, \mathcal{C}, \mathcal{R})$ be a CRN. For each reaction $C_i \rightarrow C_j \in \mathcal{R}$, we associate the **reaction vector** $C_j - C_i \in \mathbb{R}^m$. The linear subspace of \mathbb{R}^m spanned by the reaction vectors is called the **stoichiometric subspace** of \mathcal{N} , defined as $S = \text{span}\{C_j - C_i \in \mathbb{R}^m \mid C_i \rightarrow C_j \in \mathcal{R}\}$. The **rank** of \mathcal{N} is given by $s = \dim(S)$, i.e., the rank of the network is the rank of its set of reaction vectors. In this paper, we sometimes use the notation $\mathcal{N} = \{R_1, \dots, R_r\}$ where we loosely use the notation R_i to refer to either reaction i or its corresponding reaction vectors.

Two vectors $x^*, x^{**} \in \mathbb{R}^m$ are said to be **stoichiometrically compatible** if $x^* - x^{**}$ is an element of the stoichiometric subspace S . Stoichiometric compatibility is an equivalence relation that induces a partition of $\mathbb{R}_{\geq 0}^m$ or $\mathbb{R}_{> 0}^m$ into equivalence classes called the **stoichiometric compatibility classes** or **positive stoichiometric compatibility classes**, respectively, of the network. In particular, the stoichiometric compatibility class containing $x \in \mathbb{R}_{\geq 0}^m$ is the set $(x + S) \cap \mathbb{R}_{\geq 0}^m$ where $x + S$ is the left coset of S containing x . Similarly, the positive stoichiometric compatibility class containing $x \in \mathbb{R}_{> 0}^m$ is the set $(x + S) \cap \mathbb{R}_{> 0}^m$.

The **molecularity matrix** Y is an $m \times n$ matrix whose entry Y_{ij} is the stoichiometric coefficient of species X_i in complex C_j . The **incidence matrix** I_a is an $n \times r$ matrix whose entry $(I_a)_{ij}$ is defined as follows:

$$(I_a)_{ij} = \begin{cases} -1 & \text{if } C_i \text{ is the reactant complex of reaction } R_j \\ 1 & \text{if } C_i \text{ is the product complex of reaction } R_j \\ 0 & \text{otherwise} \end{cases} .$$

The **stoichiometric matrix** N is the $m \times r$ matrix given by $N = Y I_a$. The columns of N are the reaction vectors of the system. From the definition of stoichiometric subspace, we can see that S

In Example A.2, the number of linkage classes is $\ell = 1$: $\{2X_1, X_3, X_2 + X_3, 3X_4\}$; the number of strong linkage classes is $s\ell = 3$: $\{X_3, X_2 + X_3\}, \{2X_1\}, \{3X_4\}$; and the number of terminal strong linkage classes is $t = 1$: $\{X_3, X_2 + X_3\}$. X_3 and $X_2 + X_3$ are terminal complexes while $2X_1$ and $3X_4$ are nonterminal complexes.

A CRN is called **weakly reversible** if $s\ell = \ell$, **t -minimal** if $t = \ell$, **point terminal** if $t = n - n_r$, and **cycle terminal** if $n - n_r = 0$. The **deficiency** of a CRN is given by $\delta = n - \ell - s$.

For a CRN \mathcal{N} , the linear subspace of \mathbb{R}^m generated by the reactant complexes is called the **reactant subspace** of \mathcal{N} , defined as $R = \text{span}\{C_i \in \mathbb{R}^m \mid C_i \rightarrow C_j \in \mathcal{R}\}$. The **reactant rank** of \mathcal{N} is given by $q = \dim(R)$, i.e., the reactant rank of the network is the rank of its set of complexes. The **reactant deficiency** of \mathcal{N} is given by $\delta_p = n_r - q$.

To make sense of the reactant subspace R , write the incidence matrix as $I_a = I_a^+ - I_a^-$ where I_a^+ consists only of the 0's and 1's in I_a while I_a^- contains only the 0's and absolute values of the -1 's. We form the **reactant matrix** N^- (size $m \times r$) given by $N^- = YI_a^-$. The columns of N^- contains the reactant complexes of the system. From the definition of reactant subspace, we can see that R is the image of N^- , written as $R = \text{Im}(N^-)$. Observe that $q = \dim(R) = \dim(\text{Im}(N^-)) = \text{rank}(N^-)$.

The incidence matrix of the network in Example A.2 can be written as

$$I_a = I_a^+ - I_a^-$$

$$\begin{bmatrix} -1 & 0 & 0 & 0 & -1 \\ 0 & -1 & 1 & 1 & 0 \\ 1 & 1 & -1 & 0 & 0 \\ 0 & 0 & 0 & -1 & 1 \end{bmatrix} = \begin{bmatrix} 0 & 0 & 0 & 0 & 0 \\ 0 & 0 & 1 & 1 & 0 \\ 1 & 1 & 0 & 0 & 0 \\ 0 & 0 & 0 & 0 & 1 \end{bmatrix} - \begin{bmatrix} 1 & 0 & 0 & 0 & 1 \\ 0 & 1 & 0 & 0 & 0 \\ 0 & 0 & 1 & 0 & 0 \\ 0 & 0 & 0 & 1 & 0 \end{bmatrix}$$

allowing us to form the reactant matrix

$$N^- = YI_a^- = \begin{bmatrix} 2 & 0 & 0 & 0 & 2 \\ 0 & 1 & 0 & 0 & 0 \\ 0 & 1 & 1 & 0 & 0 \\ 0 & 0 & 0 & 3 & 0 \end{bmatrix}.$$

The network has reactant rank $q = \text{rank}(N^-) = 4$ and reactant deficiency $\delta_p = n_r - q = 4 - 4 = 0$.

A.2 Chemical Kinetic Systems

A **kinetics** K for a CRN $\mathcal{N} = (\mathcal{S}, \mathcal{C}, \mathcal{R})$ is an assignment to each reaction $C_i \rightarrow C_j \in \mathcal{R}$ of a rate function $K_{C_i \rightarrow C_j} : \mathbb{R}_{\geq 0}^{\mathcal{S}} \rightarrow \mathbb{R}_{\geq 0}$ such that

$$K_{C_i \rightarrow C_j}(X) > 0 \text{ if and only if } \text{supp}(C_i) \subset \text{supp}(X).$$

The system (\mathcal{N}, K) is called a **chemical kinetic system** (CKS). The **support** of complex $C_i \in \mathcal{C}$ is $\text{supp}(C_i) = \{X_j \in \mathcal{S} \mid c_{ij} \neq 0\}$, i.e, it is the set of all species that have nonzero stoichiometric coefficients in complex C_i .

A kinetics gives rise to two closely related objects: the species formation rate function and the associated ordinary differential equation system.

The **species formation rate function** (SFRF) of a CKS is given by

$$f(X) = \sum_{C_i \rightarrow C_j} K_{C_i \rightarrow C_j}(X)(C_j - C_i)$$

where X is the vector of species in \mathcal{S} and $K_{C_i \rightarrow C_j}$ is the rate function assigned to reaction $C_i \rightarrow C_j \in \mathcal{R}$. The SFRF is simply the summation of the reaction vectors for the network, each multiplied by the corresponding rate function. The **kinetic subspace** \mathcal{K} for a CKS is the linear subspace of $\mathbb{R}^{\mathcal{S}}$ defined by $\mathcal{K} = \text{span}\{\text{Im}(f)\}$. Note that the SFRF can be written as $f(X) = NK(X)$ where K the vector of rate functions. The equation $\dot{X} = f(X)$ is the **ordinary differential equation** (ODE) **system** or **dynamical system** of the CKS.

The ODE system of the CRN in Example A.2 can be written as

$$\dot{X} = \begin{bmatrix} \dot{X}_1 \\ \dot{X}_2 \\ \dot{X}_3 \\ \dot{X}_4 \end{bmatrix} = \begin{bmatrix} -2 & 0 & 0 & 0 & -2 \\ 0 & -1 & 1 & 1 & 0 \\ 1 & 0 & 0 & 1 & 0 \\ 0 & 0 & 0 & -3 & 3 \end{bmatrix} \begin{bmatrix} k_1 X_1^{f_{11}} \\ k_2 X_2^{f_{22}} X_3^{f_{23}} \\ k_3 X_3^{f_{33}} \\ k_4 X_4^{f_{44}} \\ k_5 X_1^{f_{51}} \end{bmatrix} = NK(X).$$

A zero of the SFRF is called an **equilibrium** or a **steady state** of the system. If f is differentiable, an equilibrium X^* is called **degenerate** if $\text{Ker}(J_{X^*}(f)) \cap S \neq \{0\}$ where $J_{X^*}(f)$ is the Jacobian of f evaluated at X^* and Ker is the kernel function; otherwise, the equilibrium is said to be **nondegenerate**.

A vector $X \in \mathbb{R}_{>0}^{\mathcal{S}}$ is called **complex balanced** if $K(X)$ is contained in $\text{Ker}(I_a)$ where I_a is the incidence matrix. Furthermore, if X is a positive equilibrium, then we call it a **complex balanced equilibrium**. A CKS is called **complex balanced** if it has a complex balanced equilibrium.

The reaction vectors of a CRN are **positively dependent** if, for each reaction $C_i \rightarrow C_j \in \mathcal{R}$, there exists a positive number $\alpha_{C_i \rightarrow C_j}$ such that

$$\sum_{C_i \rightarrow C_j} \alpha_{C_i \rightarrow C_j} (C_j - C_i) = 0.$$

A CRN with positively dependent reaction vectors is said to be **positive dependent**. Shinar and Feinberg [27] showed that a CKS can admit a positive equilibrium only if its reaction vectors

are positively dependent. The **set of positive equilibria** of a CKS is given by

$$E_+(\mathcal{N}, K) = \{X \in \mathbb{R}_{>0}^{\mathcal{S}} \mid f(X) = 0\}.$$

A CRN is said to **admit multiple (positive) equilibria** if there exist positive rate constants such that the ODE system admits more than one stoichiometrically compatible equilibria. Analogously, the **set of complex balanced equilibria** of a CKS (\mathcal{N}, K) is given by

$$Z_+(\mathcal{N}, K) = \{X \in \mathbb{R}_{>0}^{\mathcal{S}} \mid I_a K(X) = 0\} \subseteq E_+(\mathcal{N}, K).$$

Let F be an $r \times m$ matrix of real numbers. Define X^F by $(X^F)_i = \prod_{j=1}^m X_j^{f_{ij}}$ for $i = 1, \dots, r$.

A **power law kinetics** (PLK) assigns to each i th reaction a function

$$K_i(X) = k_i (X^F)_i$$

with **rate constant** $k_i > 0$ and **kinetic order** $f_{ij} \in \mathbb{R}$. The vector $k \in \mathbb{R}^r$ is called the **rate vector** and the matrix F is called the **kinetic order matrix**. We refer to a CRN with PLK as a **power law system**. The PLK becomes the well-known **mass action kinetics** (MAK) if the kinetic order matrix consists of stoichiometric coefficients of the reactants. We refer to a CRN with MAK as a **mass action system**.

In the ODE system of Example A.2, we assumed PLK so that the kinetic order matrix is

$$F = \begin{bmatrix} f_{11} & 0 & 0 & 0 \\ 0 & f_{22} & f_{23} & 0 \\ 0 & 0 & f_{33} & 0 \\ 0 & 0 & 0 & f_{44} \\ f_{51} & 0 & 0 & 0 \end{bmatrix}$$

where $f_{ij} \in \mathbb{R}$. If we assume MAK, the kinetic order matrix is

$$F = \begin{bmatrix} 2 & 0 & 0 & 0 \\ 0 & 1 & 1 & 0 \\ 0 & 0 & 1 & 0 \\ 0 & 0 & 0 & 3 \\ 2 & 0 & 0 & 0 \end{bmatrix}.$$

The reactions $R_i, R_j \in \mathcal{R}$ are called **branching reactions** if they have the same reactant complex. One way to check if we have identified all branching reactions is through the formula

$$r - n_r = \sum_{C_i} (|R_{C_i}| - 1)$$

where C_i is the reactant complex in $C_i \rightarrow C_j \in \mathcal{R}$, R_{C_i} is the set of branching reactions of C_i , and $|R_{C_i}|$ is the cardinality of R_{C_i} . $r - n_r = 0$ if and only if all reactant complexes are nonbranching. A CRN is called **branching** if $r > n_r$.

Note that the stoichiometric subspace S is just the set of all linear combinations of the reaction vectors, i.e., the set of all vectors in $\mathbb{R}^{\mathcal{S}}$ can be written in the form

$$\sum_{C_i \rightarrow C_j} \alpha_{C_i \rightarrow C_j} (C_j - C_i).$$

Let $L : \mathbb{R}^{\mathcal{R}} \rightarrow S$ be the linear map defined by

$$L(\alpha) = \sum_{C_i \rightarrow C_j} \alpha_{C_i \rightarrow C_j} (C_j - C_i).$$

$\text{Ker}(L)$ is the set of all vectors $\alpha \in \mathbb{R}^{\mathcal{R}}$ such that $L(\alpha) = 0$.

We say that a CRN is **concordant** if there do not exist an $\alpha \in \text{Ker}(L)$ and a nonzero $\sigma \in S$ having the following properties:

- (i) For each $C_i \rightarrow C_j \in \mathcal{R}$ such that $\alpha_{C_i \rightarrow C_j} \neq 0$, $\text{supp}(C_i)$ contains a species X for which $\text{sgn}(\sigma_X) = \text{sgn}(\alpha_{C_i \rightarrow C_j})$ where σ_X denotes the term in σ involving the species X and $\text{sgn}(\cdot)$ is the signum function.
- (ii) For each $C_i \rightarrow C_j \in \mathcal{R}$ such that $\alpha_{C_i \rightarrow C_j} = 0$, either $\sigma_X = 0$ for all $X \in \text{supp}(C_i)$, or else $\text{supp}(C_i)$ contains species X and X' for which $\text{sgn}(\sigma_X) = -\text{sgn}(\sigma_{X'})$, but not zero.

A network that is not concordant is **discordant**.

A CKS is **injective** if, for each pair of distinct stoichiometrically compatible vectors $X^*, X^{**} \in \mathbb{R}_{\geq 0}^{\mathcal{S}}$, at least one of which is positive,

$$\sum_{C_i \rightarrow C_j} K_{C_i \rightarrow C_j}(X^{**})(C_j - C_i) \neq \sum_{C_i \rightarrow C_j} K_{C_i \rightarrow C_j}(X^*)(C_j - C_i).$$

Clearly, an injective kinetic system cannot admit two distinct stoichiometrically compatible equilibria, at least one of which is positive.

A kinetics for a CRN is **weakly monotonic** if, for each pair of vectors $X^*, X^{**} \in \mathbb{R}_{\geq 0}^{\mathcal{S}}$, the following implications hold for each reaction $C_i \rightarrow C_j \in \mathcal{R}$ such that $\text{supp}(C_i) \subset \text{supp}(X^*)$ and $\text{supp}(C_i) \subset \text{supp}(X^{**})$:

- (i) $K_{C_i \rightarrow C_j}(X^{**}) > K_{C_i \rightarrow C_j}(X^*)$ implies that there is a species $X_k \in \text{supp}(C_i)$ with $X_k^{**} > X_k^*$.
- (ii) $K_{C_i \rightarrow C_j}(X^{**}) = K_{C_i \rightarrow C_j}(X^*)$ implies that $X_k^{**} = X_k^*$ for all $X_k \in \text{supp}(C_i)$ or else there are species $X_k, X'_k \in \text{supp}(C_i)$ with $X_k^{**} > X_k^*$ and $(X'_k)^{**} < (X'_k)^*$.

We say that a CKS is **weakly monotonic** when its kinetics is weakly monotonic.

Example A.3. Every MAK is weakly monotonic.

A.3 Decomposition Theory

A **covering** of a CRN is a collection of subsets $\{\mathcal{R}_1, \dots, \mathcal{R}_k\}$ whose union is \mathcal{R} . A covering is called a **decomposition** of \mathcal{N} if the sets \mathcal{R}_i form a partition of \mathcal{R} . \mathcal{R}_i defines a subnetwork \mathcal{N}_i of \mathcal{N} where $\mathcal{N}_i = (\mathcal{S}_i, \mathcal{C}_i, \mathcal{R}_i)$ such that \mathcal{C}_i consists of all complexes occurring in \mathcal{R}_i and \mathcal{S}_i has all the species occurring in \mathcal{C}_i . In this paper, we will denote a decomposition as a union of the subnetworks: $\mathcal{N} = \mathcal{N}_1 \cup \dots \cup \mathcal{N}_k$. We refer to a “decomposition” with a single “subnetwork” $\mathcal{N} = \mathcal{N}_1$ as the **trivial decomposition**. Furthermore, when a network has been decomposed into subnetworks, we can refer to the said network as the **parent network**.

A decomposition $\mathcal{N} = \mathcal{N}_1 \cup \dots \cup \mathcal{N}_k$ is **independent** if the parent network’s stoichiometric subspace S is the direct sum of the subnetworks’ stoichiometric subspaces S_i . Equivalently, the sum is direct when the rank of the parent network is equal to the sum of the ranks of the individual subnetworks, i.e.,

$$s = \sum_{i=1}^k s_i \text{ where } s_i = \dim(S_i).$$

A network decomposition $\mathcal{N} = \mathcal{N}_1 \cup \dots \cup \mathcal{N}_k$ is a **refinement** of $\mathcal{N} = \mathcal{N}'_1 \cup \dots \cup \mathcal{N}'_{k'}$ (and the latter a **coarsening** of the former) if it is induced by a refinement $\{\mathcal{R}_1, \dots, \mathcal{R}_k\}$ of $\{\mathcal{R}'_1, \dots, \mathcal{R}'_{k'}\}$.

Example A.4. If $\mathcal{N} = \mathcal{N}_1 \cup \mathcal{N}_2 \cup \mathcal{N}_3$ and $\mathcal{N}' = \mathcal{N}_2 \cup \mathcal{N}_3$, then

- $\mathcal{N} = \mathcal{N}_1 \cup \mathcal{N}_2 \cup \mathcal{N}_3$ is a refinement of $\mathcal{N} = \mathcal{N}_1 \cup \mathcal{N}'$; and
- $\mathcal{N} = \mathcal{N}_1 \cup \mathcal{N}'$ is a coarsening of $\mathcal{N} = \mathcal{N}_1 \cup \mathcal{N}_2 \cup \mathcal{N}_3$.

Appendix B The Nyman et al. Model

This section presents the system of ODEs of the insulin signaling in type 2 diabetes model of Nyman et al. [21]. It also lists in detail the definition of all the variables involved.

The system of ODEs of the Nyman et al. model are as follows:

$$\begin{aligned} \dot{X}_2 &= -k_1 X_2 - k_2 X_2 + k_6 X_4 + k_7 X_6 \\ \dot{X}_4 &= k_2 X_2 + k_3 X_3 - k_4 X_4 - k_6 X_4 \\ \dot{X}_3 &= k_1 X_2 - k_3 X_3 \\ \dot{X}_7 &= k_4 X_4 - k_5 X_7 X_{25} \\ \dot{X}_6 &= k_5 X_7 X_{25} - k_7 X_6 \\ \dot{X}_9 &= -k_8 X_7 X_9 - k_9 X_9 + k_{10} X_{10} + k_{14} X_{23} \\ \dot{X}_{10} &= k_8 X_7 X_9 - k_{10} X_{10} - k_{11} X_{10} X_{31} + k_{12} X_{22} \end{aligned}$$

$$\begin{aligned}
\dot{X}_{22} &= k_{11}X_{10}X_{31} - k_{12}X_{22} - k_{13}X_{22} \\
\dot{X}_{23} &= k_9X_9 + k_{13}X_{22} - k_{14}X_{23} \\
\dot{X}_{24} &= -k_{15}X_{10}X_{24} + k_{16}X_{25} \\
\dot{X}_{25} &= k_{15}X_{10}X_{24} - k_{16}X_{25} \\
\dot{X}_{26} &= -k_{17}X_{10}X_{26} + k_{18}X_{27} + k_{22}X_{28} \\
\dot{X}_{27} &= k_{17}X_{10}X_{26} - k_{18}X_{27} - k_{19}X_{27}X_{33} \\
\dot{X}_{28} &= -k_{20}X_{22}X_{28} + k_{21}X_{29} - k_{22}X_{28} \\
\dot{X}_{29} &= k_{19}X_{27}X_{33} + k_{20}X_{22}X_{28} - k_{21}X_{29} \\
\dot{X}_{30} &= -k_{23}X_{29}X_{30} - k_{24}X_{27}X_{30} + k_{25}X_{31} \\
\dot{X}_{31} &= k_{23}X_{29}X_{30} + k_{24}X_{27}X_{30} - k_{25}X_{31} \\
\dot{X}_{32} &= -k_{26}X_7X_{32} + k_{27}X_{33} \\
\dot{X}_{33} &= k_{26}X_7X_{32} - k_{27}X_{33} \\
\dot{X}_{34} &= -k_{28}X_{29}X_{34} - k_{29}X_{28}X_{34} + k_{30}X_{35} \\
\dot{X}_{35} &= k_{28}X_{29}X_{34} + k_{29}X_{28}X_{34} - k_{30}X_{35} \\
\dot{X}_{20} &= -k_{31}X_{20}X_{35} + k_{32}X_{21} \\
\dot{X}_{21} &= k_{31}X_{20}X_{35} - k_{32}X_{21} \\
\dot{X}_{36} &= -k_{33}X_{31}X_{36} + k_{34}X_{37} \\
\dot{X}_{37} &= k_{33}X_{31}X_{36} - k_{34}X_{37} \\
\dot{X}_{38} &= -k_{35}X_{37}X_{38} - k_{36}X_{38}X_{41} + k_{37}X_{39} \\
\dot{X}_{39} &= k_{35}X_{37}X_{38} + k_{36}X_{38}X_{41} - k_{37}X_{39} \\
\dot{X}_{40} &= -k_{38}X_7X_{40} - k_{39}X_{22}X_{40} - k_{40}X_{40} + k_{42}X_{42} \\
\dot{X}_{41} &= k_{38}X_7X_{40} + k_{39}X_{22}X_{40} + k_{40}X_{40} - k_{41}X_{41} \\
\dot{X}_{42} &= k_{41}X_{41} - k_{42}X_{42} \\
\dot{X}_{43} &= -k_{43}X_{41}X_{43} + k_{44}X_{44} \\
\dot{X}_{44} &= k_{43}X_{41}X_{43} - k_{44}X_{44}
\end{aligned}$$

where

X_2 = Inactive insulin receptors

X_3 = Insulin-bound receptors

X_4 = Tyrosine-phosphorylated receptors

X_6 = Internalized dephosphorylated receptors

X_7 = Tyrosine-phosphorylated and internalized receptors

X_9 = Inactive IRS-1

X_{10} = Tyrosine-phosphorylated IRS-1
 X_{20} = Intracellular GLUT4
 X_{21} = Cell surface GLUT4
 X_{22} = Combined tyrosine/serine 307-phosphorylated IRS-1
 X_{23} = Serine 307-phosphorylated IRS-1
 X_{24} = Inactive negative feedback
 X_{25} = Active negative feedback
 X_{26} = Inactive PKB
 X_{27} = Threonine 308-phosphorylated PKB
 X_{28} = Serine 473-phosphorylated PKB
 X_{29} = Combined threonine 308/serine 473-phosphorylated PKB
 X_{30} = mTORC1
 X_{31} = mTORC1 involved in phosphorylation of IRS-1 at serine 307
 X_{32} = mTORC2
 X_{33} = mTORC2 involved in phosphorylation of PKB at threonine 473
 X_{34} = AS160
 X_{35} = AS160 phosphorylated at threonine 642
 X_{36} = S6K
 X_{37} = Activated S6K phosphorylated at threonine 389
 X_{38} = S6
 X_{39} = Activated S6 phosphorylated at serine 235 and serine 236
 X_{40} = ERK
 X_{41} = ERK phosphorylated at threonine 202 and tyrosine 204
 X_{42} = ERK sequestered in an inactive pool
 X_{43} = Elk1
 X_{44} = Elk1 phosphorylated at serine 383.

Note that all the species are measured in %. The total concentration of each of the following sets of species is 100% at any given time: $\{X_2, X_3, X_4, X_6, X_7\}$, $\{X_9, X_{10}, X_{22}, X_{23}\}$, $\{X_{20}, X_{21}\}$, $\{X_{24}, X_{25}\}$, $\{X_{26}, \dots, X_{29}\}$, $\{X_{30}, X_{31}\}$, $\{X_{32}, X_{33}\}$, $\{X_{34}, X_{35}\}$, $\{X_{36}, X_{37}\}$, $\{X_{38}, X_{39}\}$, $\{X_{40}, X_{41}, X_{42}\}$, and $\{X_{43}, X_{44}\}$.

We observe that the system has mass action kinetics since every species in the terms of the ODEs has exponent 1.

Appendix C Summary of the Properties of INSMS and INRES

We provide in this section a table showing the different properties discussed in this paper.

Table 9 summarizes the properties of INSMS and INRES.

Table 9: Summary of the properties of INSMS and INRES

Property Class	INSMS	INRES
Network	Branching	
	Closed	
	High reactant diversity	
	Non-cycle terminal	
	Non-point terminal	
	Not (weakly) reversible	
	Positive dependent	
	t -minimal	
	10 subnetworks Nonconservative Concordant 5 subnetworks with $\delta = 0$ 9 subnetworks with $s = 1$ 0 subnetworks with $\delta_\rho = 0$	12 subnetworks Conservative Discordant 0 subnetworks with $\delta = 0$ 8 subnetworks with $s = 1$ 12 subnetworks with $\delta_\rho = 0$
	Structo-Kinetic	No complex balanced equilibria
Kinetic and stoichiometric subspaces coincide		
Monostationary		
Injective Monostationary in all weakly monotonic systems		Non-injective Multistationary for some weakly monotonic systems
Kinetic	Nondegenerate equilibria	
	8 ACR species	No ACR species